Journal of Modern Optics

ISSN: 0950-0340 (Print) 1362-3044 (Online) Journal homepage: https://www.tandfonline.com/loi/tmop20

Thermal nonlinear optical response of meso-tetraphenylporphyrin under aggregation conditions versus that in the absence of aggregation

Saifollah Rasouli, Fereshteh Sakha, Aida G. Mojarrad & Saeed Zakavi

To cite this article: Saifollah Rasouli, Fereshteh Sakha, Aida G. Mojarrad & Saeed Zakavi (2018) Thermal nonlinear optical response of meso-tetraphenylporphyrin under aggregation conditions versus that in the absence of aggregation, Journal of Modern Optics, 65:8, 1009-1017, DOI: 10.1080/09500340.2017.1418442

To link to this article: https://doi.org/10.1080/09500340.2017.1418442

JOURNAL OF MODERN OPTICS, 2018
VOL. 65, NO. 8, 1009–1017
https://doi.org/10.1080/09500340.2017.1418442

Taylor & Francis
Taylor & Francis Group

Thermal nonlinear optical response of meso-tetraphenylporphyrin under aggregation conditions versus that in the absence of aggregation

Saifollah Rasouli[a,c], Fereshteh Sakha[a], Aida G. Mojarrad[b] and Saeed Zakavi[b]

[a]Department of Physics, Institute for Advanced Studies in Basic Sciences (IASBS), Zanjan, Iran; [b]Department of Chemistry, Institute for Advanced Studies in Basic Sciences (IASBS), Zanjan, Iran; [c]Optics Research Center, Institute for Advanced Studies in Basic Sciences (IASBS), Zanjan, Iran

ABSTRACT

In this work, measurement of thermally induced nonlinear refractive index of meso-tetraphenylporphyrin (H_2TPP) at different concentrations in 1,2-dicoloroethane using a double-grating interferometer set-up in a pump–probe configuration is reported. The formation of aggregates of H_2TPP at concentrations greater than ca. 5×10^{-5} M was evident by deviation from Beer's law. An almost focused pump beam passes through the solution. A part of the pump beam energy is absorbed by the sample and therefore a thermal lens is generated in the sample. An expanded probe beam propagates through the sample and indicates the sample refractive index changes. Just after the sample a band-pass filter cuts off the pump beam from the path but the distorted probe beam passes through a double-grating interferometer consisting of two similar diffraction gratings with a few centimetres distance. A CCD camera is installed after the interferometer in which on its sensitive area two diffraction orders of the gratings are overlying and producing interference pattern. The refractive index changes of the sample are obtained from the phase distribution of the successive interference patterns recorded at different times after turning on of the pump beam using Fourier transform method. In this study, for different concentrations of H_2TPP in 1,2-dichloroethane solution the thermal nonlinear refractive index is determined. Also, we present the measurement of the temperature changes induced by the pump beam in the solution. We found that value of nonlinear refractive index increased by increasing the concentration up to a concentration of 5×10^{-4} M and then decreased at higher concentrations. In addition, we have investigated the stability of the observed thermal nonlinearity after a period of two weeks from the sample preparation.

ARTICLE HISTORY
Received 25 August 2017
Accepted 7 December 2017

KEYWORDS
Meso-tetraphenylporphyrin (H_2TPP); self-aggregation; thermal lens; nonlinear refractive index; double gratings interferometer; pump–probe arrangement

Introduction

Porphyrins and derivatives as a class of conformationally flexible aromatic compounds have been the subject of many photo physical studies due to their unique absorption and emission spectra in the visible and ultraviolet region (*1*, *2*). Indeed, applications of porphyrins in different fields such as photodynamic therapy and their photosensitizing efficiency depend on the absorption cross-sections, lifetimes and quantum yields of the excited states of the aromatic macrocycle (*3*). After the first report on the nonlinear optical behaviour of meso-tetraphenylporphyrin (H_2TPP) and its Co(II) and Zn(II) complexes by W. Blau et al. in 1985, the non-linear optics of porphyrins and metalloporphyrins have been extensively studied (*4*–*7*). A decrease in the transmission of dye samples with increase in the incident light intensity known as reverse saturable absorption occurs when the absorption cross-section from the excited state up to a higher excited state is more intense than the absorption from the ground state to the excited state (*8*). This optical behaviour can be used to prepare information on the dynamic response and photo physical properties of the dye molecules (*7*, *8*). Many physicochemical properties of porphyrins are influenced by H and J aggregation of porphyrins. Different systems, such as light harvesting antennas of photosynthetic plants and bacteria utilize the aggregated species. Also, the optical features of porphyrin aggregates can be potentially exploited for their nonlinear optical properties. The formation of porphyrin aggregates is accompanied with the shift in the energy of the excited states of porphyrins which in turn leads to red or blue shift of the absorption bands (*9*, *10*). In the present study the nonlinear optical properties of H_2TPP (Figure 1) in the presence and absence of self-aggregation have been studied and

CONTACT Saifollah Rasouli rasouli@iasbs.ac.ir

compared. It is noteworthy that in this study, an investigation on the thermally induced nonlinear refractive index of the title porphyrin in 1,2-dichloroethane is presented using a double-grating interferometer setup in a pump–probe configuration (*11*).

It is noteworthy that H_2TPP has been used as a representative porphyrin of a series of aromatic and fully conjugated macrocyclic compound to conduct the nonlinear optical experiments based on the proposed technique. Furthermore, the results seem to have potential applications in designing nonlinear optics devices on the basis of porphyrin aggregates.

In this work, in parallel to determining thermal nonlinear optical response of meso-tetraphenylporphyrin under aggregation conditions, for the first time, determining refractive index and temperature changes in the sample during the sample evolution is reported. We present a detailed procedure for determining the temperature changes induced by the pump beam inside the sample.

It is worth mentioning that, in this work for the first time we propose the use of double-grating interferometry technique for study of the fluid dynamic induced by a thermal lens. The double-grating interferometry technique is very suitable for investigating the behaviour of samples whose characteristics vary with time. It is know that, in the well-known Z-scan method, due to the scanning time of the sample along the optical axis, it is a time consuming method. Therefore, for investigation of dynamic phenomena, such as the case we are reporting in this work, it is impossible to use the Z-scan method for the measurements of refractive index and temperature changes during the sample evolution that can be induced by turn on or changing pump laser power or other parameters. Unlike the Z-scan technique, our method can be used almost in real-time. Also, it is possible to record a sequence of successive interference patterns in real time then the data can be analyzed in a postponed time. But, for the Z-scan method, it is almost impossible to record data of Z-scan for all stages of changes when sample has a dynamic behavior.

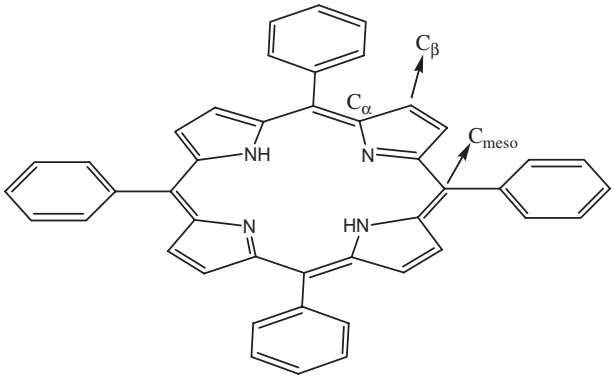

Figure 1. *Meso*-tetraphenylporphyrin, H_2TPP.

Furthermore, oncomparing to the Z-scan method, double-grating interferometry is relatively insensitive to the alignment of the measurement beam. On the other hand, in comparing with the other interferometry methods, the arrangement of the technique is very simple and stable. Finally, the ease of the implementation of the measurement technique is comparable to the Z-scan method.

In the set-up, an almost focused pump beam is propagated through the sample, some part of its energy is absorbed by the sample, and it deduces a thermal lens in the sample. Any changes of the sample's refractive index are indicated by an expanded probe beam. The phase distortions induced by the sample on the probe beam are determined by a double-grating interferometer. The refractive index changes are obtained from the phase distribution of the interference patterns. Phase maps of the interference fringe patterns are obtained using Fourier transform method. In this study, for different concentrations of H_2TPP, measurements are processed to investigate the effect of concentration on the nonlinear refractive index of H_2TPP. It is shown that for H_2TPP the value of nonlinear refractive index increases by increasing H_2TPP concentration from 10^{-6} up to 5×10^{-4} M then its value decreases at higher concentrations. Furthermore, a good stability for the observed thermal nonlinearity in most of the concentrations after two weeks from the preparation of the samples is seen.

Experimental setup

For the measurements of thermal nonlinearity of different concentrations of the sample, a lateral shearing interferometer set-up by the aid of two diffraction gratings, as shown in Figure 2 is used. G1 and G2 are two similar gratings that are illuminated with an expanded plane beam called probe beam. A pump laser beam is propagated collinearly with the expanded plane probe beam by use of a dichroic mirror. These beams pass through the sample, while just after the sample using a suitable band-pass filter the pump beam is completely absorbed and removed from the path. By the thermally induced sample the probe beam is distorted and it passes through the double-grating interferometer. Lateral shearing interference pattern is generated by the gratings can be recorded by use of a CCD camera. In the experiment, successive interference patterns from a bit moment before the turning on of the pump beam till to a time a stable condition is occurred for the fringes patterns, are recorded by the camera and after digitization have been stored in a computer. For a given time after turning on of the pump beam, by use of a pair of shearing interferograms captured, respectively, before passing the pump beam through the sample and at the desired time after turning on of the pump beam,

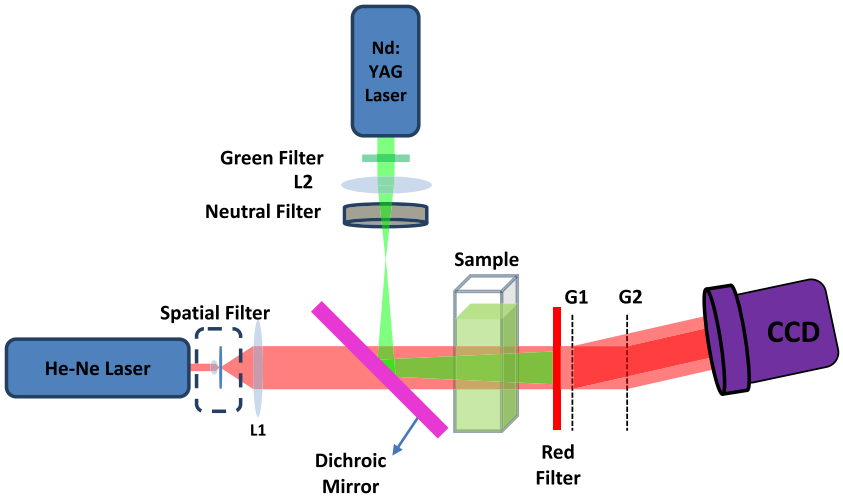

Figure 2. Schematic diagram of the experimental setup, L1, L2, G1, and G2, are focusing lens, collimating lens, first grating and second grating, respectively.

the refractive index changes are determined. Phase maps of the successive interference patterns are obtained by the Fourier transform algorithm. By subtraction of these phase maps from that of the fringes pattern captured before passing the pump beam, the sample phase maps can be determined at the given time. From that, thermal nonlinear refractive index of the sample and temperature changes at the recording times of the interference patterns can be calculated. Detail theoretical and experimental considerations concerning the double-grating interferometer setup for the thermal nonlinear refractive index measuring was presented in the reference (*11*).

Preparation of H_2TPP

H_2TPP was prepared by the reaction of freshly distilled pyrrole (0.08 mol, 5.6 ml) and benzaldehyde (0.08 mol, 8 ml) in refluxing propionic acid (300 ml) and purified according to the literature (*12*). ^1H NMR (400 MHz, $CDCl_3$, TMS), δ/ppm: -2.77 (2H, br, s, NH), 7.77–7.84 ($8H_m$ and $4H_p$, m), 8.26–8.27 ($8H_o$, d), 8.90 ($8H_\beta$, s); ^{13}C NMR (400 MHz, $CDCl_3$, TMS), δ/ppm: 120.18 (C_{meso}), 142.20 (C_1), 134.60 (C_2, C_6), 126.73 (C_3, C_5), 127.75 (C_4), 131.5 (C_β); UV-vis in CH_2Cl_2, λ_{max}/nm (log ε): 417 (5.79), 513 (4.58), 548 (4.38), 590 (4.30), 645 (4.29).

Aggregation of H_2TPP

Previous studies showed that H_2TPP forms aggregates at concentrations greater than ca. 10^{-6} M (*13, 14*). However, the type and polarity of solvent play a key role in the exact concentration needed for the initiation of the aggregation process. The plot of absorbance versus concentration has been used to provide evidence on the formation of porphyrin aggregates. Indeed, considerable deviation from linearity (deviation from Beer's law) occurs upon the formation of porphyrin aggregates (*14*). It is noteworthy that deviation from Beers law may be due to different causes including the limitations of Beers law (mainly its limitations at high concentrations), chemical phenomenon (association or dissociation of the analyst molecules) and instrumental limitations (*15–17*).The deviation from linearity observed in this study was attributed to the aggregation of porphyrins that is a well-known intermolecular interaction between porphyrin molecules at relatively high concentration of porphyrins (*13, 14, 18, 19*). In Figure 3 UV-visible spectral changes upon the increase in H_2TPP concentration from 10^{-6}–5×10^{-3} M in 1,2-dichloroethane are shown.

The dashed curve (C = 10^{-4} M) shows the approximate concentration required for aggregation of H_2TPP. It is noteworthy that the formation of porphyrin aggregates leads to the broadening of the Soret band due to the red and/or blue shifts of this band; the formation of H and J aggregates shifts the Soret band to lower and higher wavelengths, respectively (*9, 10, 19*). The dynamics of the shifts in the absorption bands of aggregates have been explained on the basis of theory of the excitonic splitting. Porphyrin H-aggregates consist of parallel orientation of monomers which leads to a transition to the upper excited state (parallel orientation of transition dipoles) and the blue shift of the corresponding absorption band. On the other hand, the head-to-tail arrangement of monomers in J-aggregates leads to a transition to a lower excited state (anti-parallel orientation of transition dipoles) and consequently the red shift of the band (*20, 21*).

In order to determine the exact concentration in which the aggregation occurs, the absorbance vs. concentration

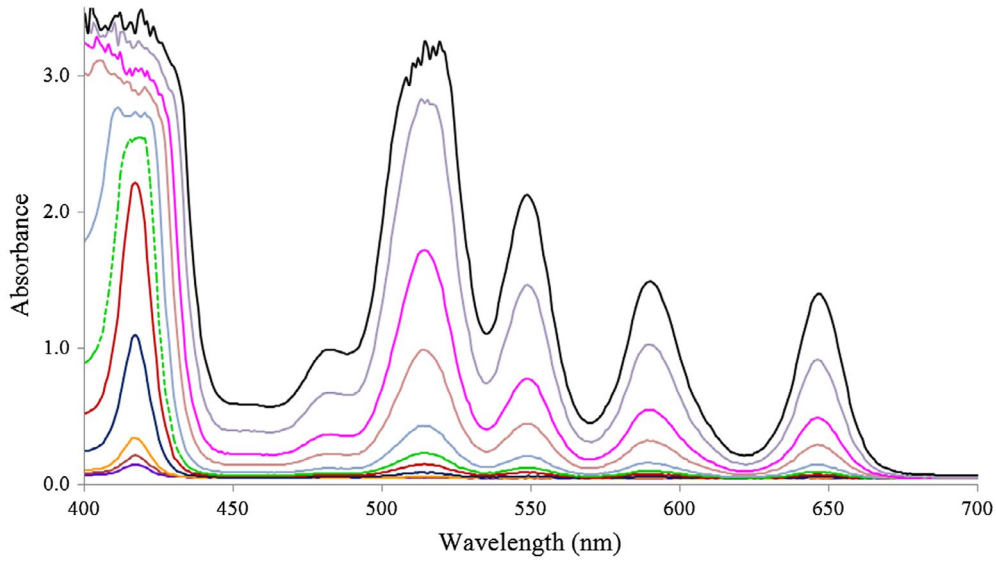

Figure 3. Visible spectral changes upon the increase of H_2TPP concentration from 10^{-6} (violet curve) to 5×10^{-3} M (black curve) in 1,2-dichloroethane. The dashed green curve ($C = 10^{-4}$ M) shows the minimum concentration required for aggregation of H_2TPP.

(the Beer law experiment) is plotted for H_2TPP (Figure 4). It is observed that departure from linearity occurs at concentrations greater than ca. 5×10^{-5} M.

Figure 4 demonstrates the changes in the UV-visible spectrum of H_2TPP caused by increasing the porphyrin concentration. The broadening of the Soret band (red curve) occurs at a concentration of 10^{-4} M that is very close to the concentration in which departure from linearity was observed (Figure 3).

Optical measurements and results

In this section, details of the measurement process of the thermal nonlinear refractive index n_2 of H_2TPP in 1,2-dichloroethane by the double-grating interferometry are presented. Also, we present the measurement of the temperature changes inside the sample induced by the pump beam.

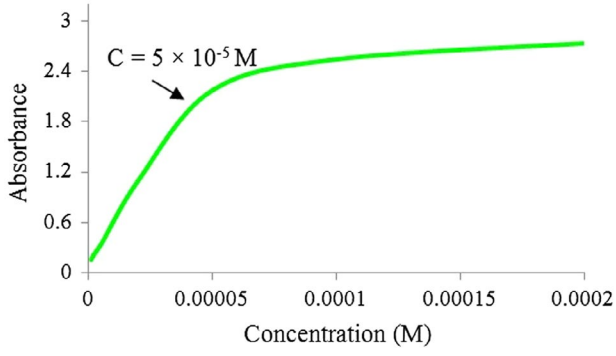

Figure 4. Beer law experiment for H_2TPP in 1,2-dichloroethane at room temperature.

In this paper, we refer to the measurements which were performed on different concentration of H_2TPP in 1, 2-dichloroethane, in a 3.5 mm thickness cell. Light from a He–Ne laser with wavelength $\lambda = 632.8$ nm with power 5 mW was first passed through a beam expander and a spatial filtering unit. A collimating lens of focal length 160 mm and diameter 60 mm was used to collimate probe laser beam. The second harmonic of a 50 mW cw diode-pumped Nd:YAG laser beam at 532 nm is aligned collinearly with the collimated probe beam by a dichroic mirror. These beams pass through the sample. Right behind the sample using a suitable band-pass filter the pump beam is intercepted but the probe beam strikes G1. The distance between the planes of G1 and G2 is chosen as 70 mm. Gratings G1 and G2 with a period of 1/100 mm were installed on suitable mounts. The holders of the gratings can be rotated around the optical axis to adjust the angle between the gratings. The sheared interferograms were recorded by a charge-coupled device CCD detector (The DCC1545 M-GL THORLABS) having 1024×1280 pixels with each pixel area 5.5×5.5 μm^2.

In Figure 5, in the first row from the left to right, three typical shearing interference patterns, respectively before the pump beam illumination, after the pump beam illumination at the maximum state of fringes' deformations, and at the stable state of fringes' deformations are shown. Their corresponding phase maps are shown in the second row and the pure phase maps correspond to the deformations induced by the thermal lens on the fringes maps are given in the third row. At the recoding of the patterns, the pump beam power was 2 mW, the concentration of H_2TPP in 1,2-dichloroethane was 10^{-5} M, and the interference

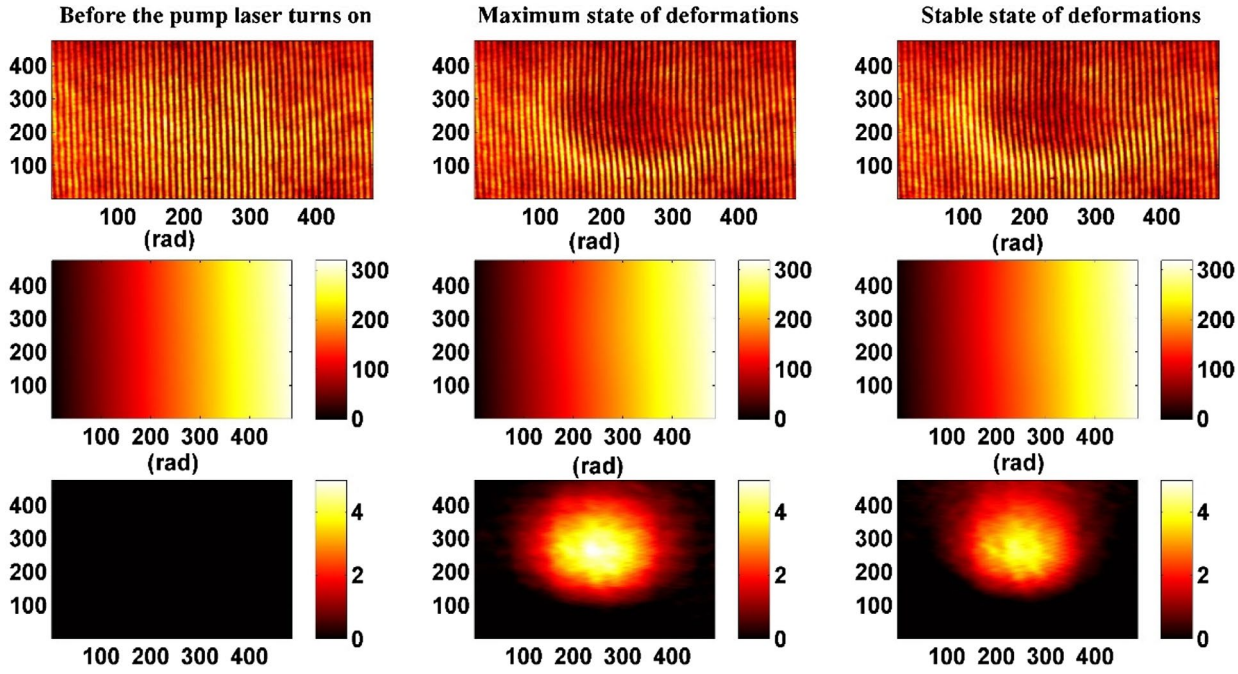

Figure 5. Typical shearing interference patterns recorded, respectively, before the pump beam illumination, after the pump beam illumination at the maximum state of fringes' deformations, and at the stable state of fringes' deformations are shown in the first row from the left to right. In the second row their corresponding phase maps are shown. In the third row the pure phase maps correspond to the deformations induced by the thermal lens on the fringes maps are shown. The pump beam power was 2 mW, the concentration of H_2TPP in 1,2-dichloroethane was 10^{-5} M, and the interference pattern of the stable state was recorded about 34 s after turning on of the pump beam.

pattern of the stable state was recorded about 34 s after turning on of the pump beam.

Evolutions of refractive index profiles after turning on of the pump beam for a 10^{-5} M solution of H_2TPP in 1,2-dichloroethane are shown in Figure 6. The time of recoding of the patterns from the moment of the turning on of the pump beam are written above each of the maps.

In Figure 7 refractive index profiles, along lines consist the maximum values of the refractive index changes for the 2D maps of Figure 6, are illustrated.

The pure phase map, $\Delta\varphi$, corresponds to the deformations induced by the thermal lens on the fringe map is calculated by difference of the phase map of the fringes at a given time after turning on of the pump beam and the phase map of the fringes captured before passing the pump beam through the sample. Refractive index changes in the sample at a given time is obtained using (*11*)

$$\Delta n = \frac{\lambda}{2\pi L}\Delta\varphi, \tag{1}$$

where λ is wavelength and L is the sample length. Now using following relation one can estimate temperature changes inside the sample at given times after passing pump beam:

$$\Delta n = \frac{dn}{dT}\Delta T. \tag{2}$$

For calculation of the temperature changes, according Equation (2), we need to have the thermo-optical coefficient of the sample, $\frac{dn}{dT}$. This coefficient can be determined by an experimentally measurement of the refractive index of the sample at various temperatures. For the dichloroethane solution this changes are given in Figure 8.

It is mentioning that due to the very low concentrations of H_2TPP (10^{-6} to 5×10^{-3} M) the data of Figure 8 are more or less valid for the 1,2-dichloroethane solutions of H_2TPP.

Now using Equations 1 and 2 and the pure phase maps of the successive frames, the sample temperature changes can be determined at successive frames were recorded at different times from the moment of turning on of the pump beam. In Figure 9 calculated temperature changes for a 10^{-5} M solution of H_2TPP in 1,2-dichloroethane after turning on of the pump beam are presented.

With a pump beam power of 2 mW, a maximum temperature change of ca. 0.25 K is measured. As it is seen in Figure 9, by passing the pump beam through the sample, temperature of the sample increased rapidly in a few second time interval, reaches to a maximum value, decreases slightly, and gets an almost constant value. This phenomenon can be interpreted by considering the effect of particle displacement in the opto-thermally induced temperature gradient in the sample that is well-known as the Soret effect. Further consideration concerning this

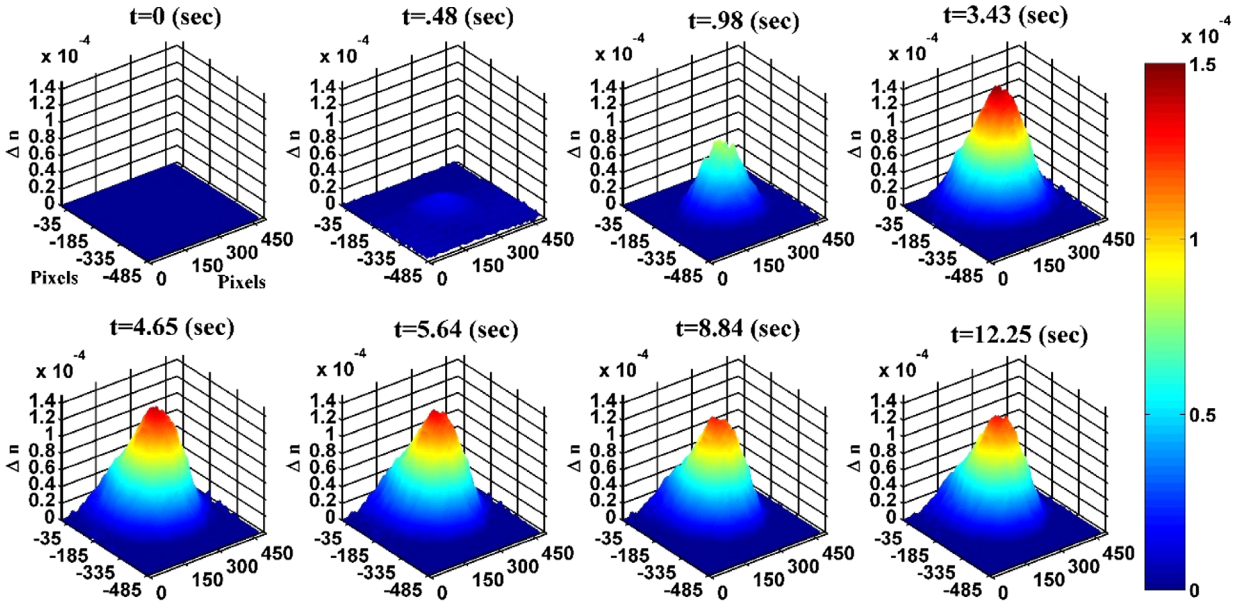

Figure 6. Evolutions of refractive index profiles after turning on of the pump beam for the concentration 10^{-5} M of H_2TPP in 1,2-dichloroethane solution. The time is written above each of the maps shows the recoding time of the pattern from the moment of the turning on of the pump.The pump beam power was 2 mW.

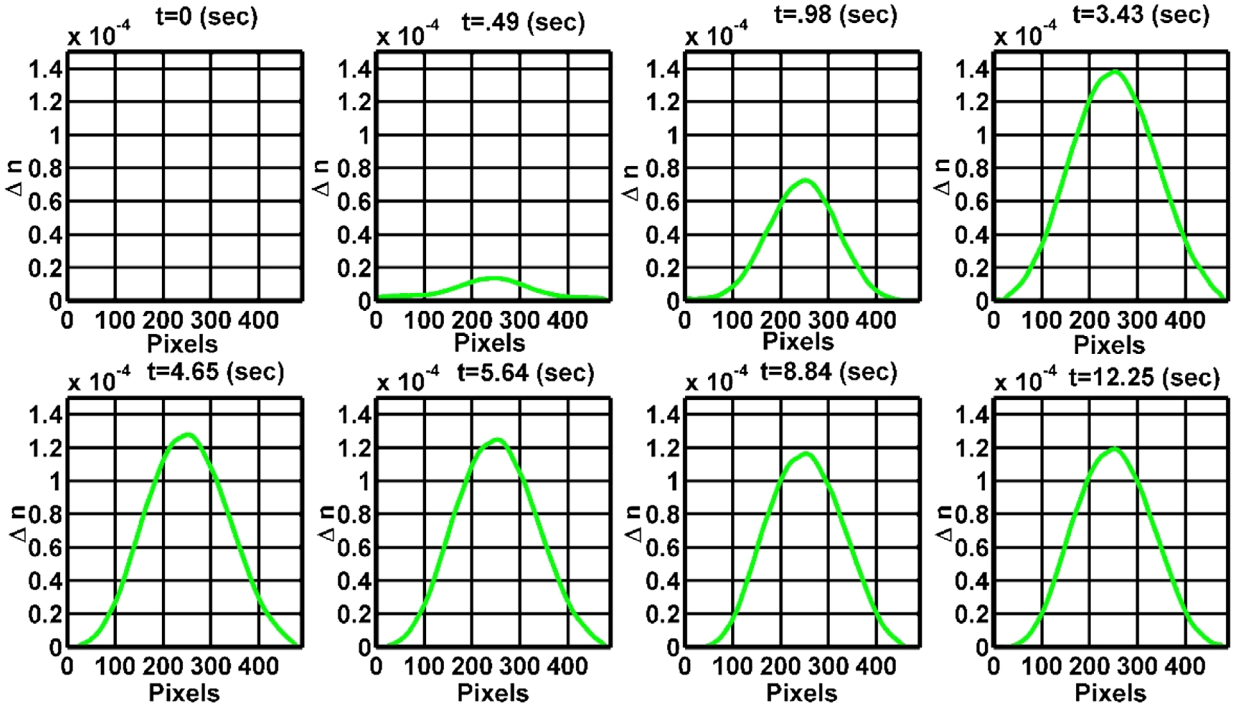

Figure 7. Refractive index profiles along lines consisting maximum values of refractive index changes for 2D maps are shown in Figure 6.

phenomenon, is the subject of another work in our group which will be appeared other place.

In Table 1, the measured data for the nonlinear refractive index of the 1,2-dichloroethane solution at different concentrations of H_2TPP are presented. For given concentrations of the sample, two sets of data were prepared after 2 days and after 14 days from the samples preparation. For each measurement, the used pump beam power is presented.

Based on the data of Table 1, in Figure 10, the maximum values of the measured induced refractive indexes for different concentrations of H_2TPP are plotted for two sets of measurements performed on the same sample, two days and two weeks after the preparation of the samples,

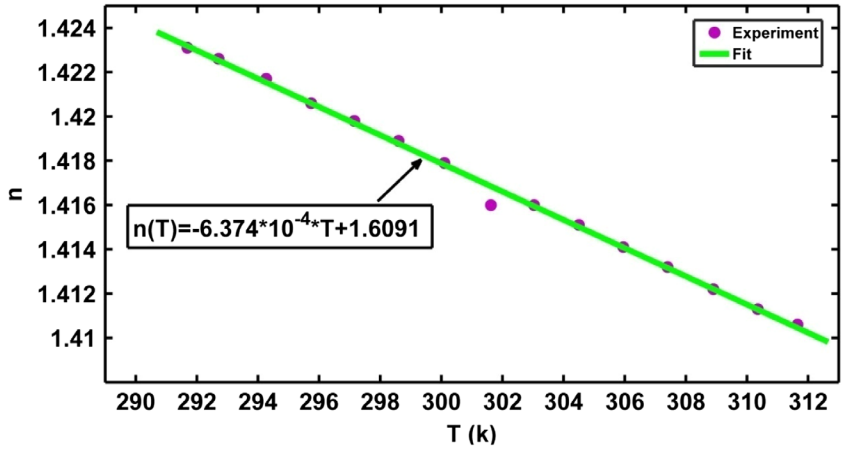

Figure 8. Refractive index changes in 1,2-dichloroethane as a function of temperature (*22*).

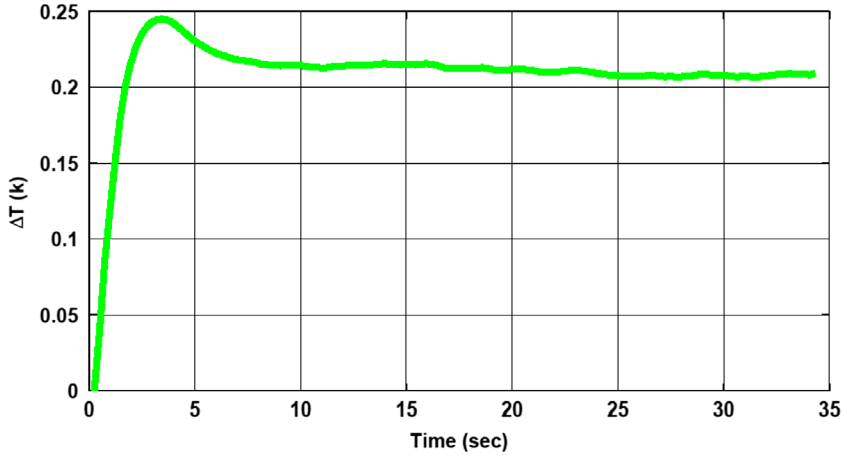

Figure 9. Calculated temperature changes after turning on of the pump beam with a power of 2 mW for a 10^{-5} M solution of H_2TPP in 1,2-dichloroethane.

Table 1. Nonlinear refractive index for different concentrations of H_2TPP

	Measurements were done on the samples after 2 days from the sample preparation				Measurements were done on the same samples after 14 days from the sample preparation			
H_2TPP Concentration	Power (mW)	Δn (×10^{-4})	n2 (cm2/W) (×10^{-4})	Error (%)	Power (mW)	Δn (×10^{-4})	n2 (cm2/W) (×10^{-4})	Error (%)
10^{-6}	50	0.385	0.0226±0.001	4.42	50	0.324	0.02±0.0017	8.5
2×10^{-6}	50	0.572	0.0435±0.0022	5.05	50	0.523	0.053±0.0023	4.339
5×10^{-6}	50	1.635	0.068±0.0023	3.38	50	1.535	0.119±0.0039	3.277
10^{-5}	20.5	1.349	0.266±0.0039	1.46	19.3	1.363	0.272±0.00624	2.294
2×10^{-5}	13.8	1.573	0.429±0.013	3.03	11.5	1.473	0.474±0.01	2.109
5×10^{-5}	4.04	1.163	1.04±0.022	2.11	3.67	1.1016	1.09±0.0457	4.192
10^{-4}	3.6	1.613	1.6±0.042	2.62	3.4	1.4732	1.6±0.053	3.312
2×1^{-4}	3.7	2.37	2.5±0.29	11.6	1.8	1.3658	2.7±0.083	3.074
5×10^{-4}	1.64	1.582	3.6±0.1	2.77	1.6	1.3658	3.11±0.112	3.601
10^{-3}	1.59	1.611	3.2±0.077	2.40	1.5	1.5737	3.925±0.17	4.331
2×10^{-3}	1.6	1.34	3.1±0.05	1.61	1.5	1.4628	3.6±0.115	3.194
5×10^{-3}	2	1.267	2.27±0.11	4.84	1.5	1.3818	3.4±0.127	3.735

respectively. As it appears from Figure 10, after two weeks, a good stability for the observed thermal nonlinearity is observed in most of the porphyrin concentrations. It is worthy to mention that, Porphyrins as photosensitizers can catalyze the aerobic photooxidation of different organic compounds as well as themselves (*23, 24*). Accordingly, ageing of porphyrin solution in the presence of molecular oxygen and visible light may lead to partial decomposition

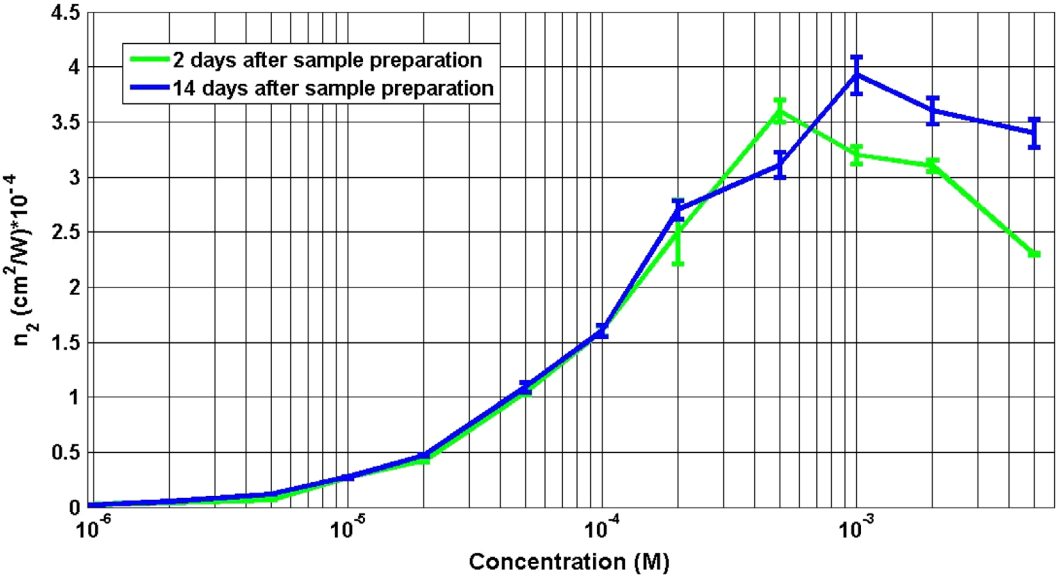

Figure 10. Maximum values of the measured induced refractive index at different concentrations of H_2TPP. Two series of the measurements were done on the same samples after 2 and 14 days from the sample preparation.

of porphyrins. Also, degree of aggregation of porphyrins and the size of porphyrin assemblies depends on the ageing time. The results of this study show that the porphyrin solutions are stable at least for ca. two weeks. Further ageing needs the removal of oxygen from the porphyrin solution. Furthermore, the solution should be kept under dark conditions.

It should be mentioned that, in the measurements, fluctuations of the pump and probe laser powers were about 2% that were considered in the error analysis.

Because in the measurement method, from the comparison of the probe beam phases at an area that the pump beam passes through the sample and at an area considerably away from the path of the pump beam, refractive index and temperature changes are determined, accessing to an environmentally stable lab is not necessary. Though, we have prepared a thermally stable condition for the lab as possible as.

Conclusion

In this work, for the first time, we proposed the use of double-grating interferometry technique for study of fluid dynamic induced by a thermal lens. By the proposed method, as it is a timesaving method, any changes in the refractive index and temperature of a given sample that can be induced by different physical or chemical processes are measurable. In this paper, we have presented a detailed procedure for determining the temperature changes induced by the pump beam inside the sample. A maximum temperature changes of ca. 0.25 K with a pump beam power of 2 mW was measured for a 10–5 M solution of H2TPP in 1,2-dichloroethane. In parallel, we have measured the thermal nonlinear refractive index of H2TPP in 1,2-dichloroethane. In this work, a detailed investigation on the thermal nonlinear properties of H_2TPP in 1,2-dicoloroethane using the double-grating interferometer set-up is presented. Influence of the self-aggregation on the thermal nonlinear optical response of H_2TPP at different concentrations is manifested. It was found that the value of nonlinear refractive index of H_2TPP increases by increasing its concentration up to 5×10^{-4} M and then decreases at higher concentrations. The refractive index of the dichloroethane solution of H_2TPP was found to be depended on the concentration of the used porphyrin. Beer law experiment for H_2TPP revealed that self aggregation of H_2TPP occurs at concentrations greater than ca. 5×10^{-4} M. After this concentration, self aggregation of H_2TPP leads to the formation of H and J aggregates. Accordingly, the refractive index measured after 5×10^{-4} M belongs to the porphyrin aggregates rather than the single molecules dissolved in dichloroethane. Finally, the stability of the observed thermal nonlinearity for a period of two weeks after the preparation of the samples was verified.

Acknowledgments

We would like to thank Dr. Mohammad Yeganeh for his kind help.

Disclosure statement

No potential conflict of interest was reported by the authors.

ORCID

Saifollah Rasouli http://orcid.org/0000-0003-2703-8925

References

(1) Harvey, P.D. In *The Porphyrin Handbook: Multporphyrins, Multiphthalocyanines and Arrays*; Kadish, K., Guilard, R., Smith, K.M.,Eds.; Academic Press: Boston, 2000, Vol. 18; pp 63–243.

(2) Blau, W.; Byrne, H.; Dennis, W.M.; Kelly, J.M. Reverse Saturable Absorption in Tetraphenylporphyrins. *Optics Comm.* **1985**, *56*, 25–29. doi:10.1016/0030-4018(85)90059-8.

(3) DeRosa, M.C.; Crutchley, R.J. Photosensitized Singlet Oxygen and its Applications. *Coord. Chem. Rev.* **2002**, *233*, 351–371. doi:10.1016/S0010-8545(02)00034-6.

(4) Blau, W.; Reber, R.; Penzkofer, A. S_1-S_0 Relaxation Time of Saturable Absorber DDI. *Optics Comm.* **1982**, *43*, 210–214. doi: 10.1016/0030-4018(82)90348-0.

(5) Merhi, A.; Grelaud, G.; Green, K.A.; Minh, N.H.; Reynolds, M.; Ledoux, I.; Barlow, A.; Wang, G.; Cifuentes, M.P.; Humphrey, M.G.; Paul, F.; Paul-Roth, C.O. A Hybrid Ruthenium Alkynyl/Zinc Porphyrin "Cross Fourchée" with Large Cubic NLO Properties. *Dalton Trans.* **2015**, *44*, 7748–7751. doi:10.1039/C5DT00768B.

(6) Swain, D.; Rana, A.; Panda, P.K.; Rao, S.V. Strong Two-Photon Absorption Properties and Ultrafast Pump-Probe Studies of Novel Porphyrin Derivatives. *Chem. Phys. Lett.* **2014**, *610–611*, 310–315. doi:10.1016/j.cplett.2014.07.013.

(7) Senge, M.O.; Fazekas, M.; Notaras, E.G.A.; Blau, W.J.; Zawadzka, M.; Locos, O.B.; Ni, E.M. Mhuircheartaigh, "Nonlinear Optical Properties of Porphyrins". *Adv. Mater.* **2007**, *19*, 2737–2774. doi:10.1002/adma.200601850.

(8) Blau, W.; Dankesreiter, W.; Penzkofer, A. Saturable Absorption of Dyes Excited to the Long-Wavelength Region of the S0-S1 Absorption Band. *Chem. Phys.* **1984**, *85*, 473–479. doi: 10.1016/0301-0104(84)85273-8.

(9) Rosa, A.; Ricciardi, G.; Baerends, E.J.; Romeo, A.; Scolaro, L.M. Effects of Porphyrin Core Saddling, Meso-Phenyl Twisting, and Counterions on the Optical Properties of Meso-Tetraphenylporphyrin Diacids: The [H4TPP](X)2 (X = F, Cl, Br, I) Series as a Case Study. *J. Phys. Chem. A* **2003**, *107*, 11468–11482. doi:10.1021/jp030999n.

(10) Zakavi, S.; Hoseini, S. The Absorption and Fluorescence Emission Spectra of *Meso*-Tetra (Aryl) Porphyrin Dications with Weak and Strong Carboxylic Acids: a Comparative Study. *RSC Adv.* **2015**, *5*, 106774–106786. doi:10.1039/C5RA20445C.

(11) Rasouli, S.; Ghorbani, M. Nonlinear refractive index measuring using a double-grating interferometer in pump–probe configuration and Fourier transform analysis, *J. Opt*. **2012**, 14, 035203 (6pp). https://doi.org/10.1088/2040-8978/14/3/035203

(12) Adler, A.D.; Longo, F.R.; Finarelli, J.D.; Goldmacher, J.; Assour, J.; Korsakoff, L. A Simplified Synthesis for Meso-Tetraphenylporphine. *J. Org. Chem.* **1967**, *32*, 476. doi:10.1021/jo01288a053.

(13) Castricianoa, M.A.; Romeoa, A.; Scolaro, L.M. Aggregation of Meso-Tetrakis (4-sulfonatophenyl) Porphyrin on Polyethyleneimine in Aqueous Solutions and on a Glass Surface. *J. Porphyrins Phthalocyanines* **2002**, *6*, 431–438. doi:10.1142/S1088424602000531.

(14) Pasternack, R.F.; Huber, P.R.; Boyd, P.; Engasser, G.; Francesconi, L.; Gibbs, E.; Fasella, P.; Venturo, G.C. Aggregation of Meso-Substituted Water-Soluble Porphyrins. *J. Am. Chem. Soc.* **1972**, *94*, 4511–4517. doi:10.1021/ja00768a016.

(15) Douglas, A.; Skoog, D.A.; Holler F.J. *Analytical Chemistry: An Introduction*, 7th ed.; 1999.(Saunders Golden Sunburst Series)

(16) Skoog, D.A.; West, D.M.; Holler, F.J.; Crouch, S.R. *Fundamentals of Analytical Chemistry*, 9th ed.; 2013; pp 669–671.

(17) Harvey, D. *Modern Analytical Chemistry*; McGraw-Hill, Higher Education, 2000; pp 386.

(18) Kuba′t, P.; Lang, K.; Procha′zkova′, K.; Anzenbacher, P. Self-Aggregates of Cationic Meso-Tetratolylporphyrins in Aqueous Solutions. *Langmuir* **2003**, *19*, 422–428. doi:10.1021/la026183f.

(19) Luca, G.D.; Romeo, A.; Scolaro, L.M. Counteranion Dependent Protonation and Aggregation of Tetrakis (4-sulfonatophenyl) Porphyrin in Organic Solvents. *J. Phys. Chem. B* **2006**, *110*, 7309–7315. doi:10.1021/jp0530348.

(20) Knapp, E.W. Line Shapes of Molecular Aggregates, Exchange Narrowing and Intersite Correlation. *Chem. Phys.* **1984**, *85*, 73–82. doi:10.1016/S0301-0104(84)85174-5.

(21) Hollingsworth, J. A study of the Self-Assembly of Water-Soluble Porphyrins in Aqueous Solution. (2009), LSU Master's Theses, 2001; pp 7. http://digitalcommons.lsu.edu/gradschool_theses/2001.

(22) Valkai, S.; Liszi, J.; Szalaic, I. Temperature Dependence of the Refractive Index for Three Chloromethane Liquids at 514.5 nm and 632.8 nm Wavelengths. *J. Chem. Thermodynamics* **1998**, *30*, 825–832. doi:10.1006/jcht.1998.0349.

(23) Zakavi, S.; Hoseini, S.; Mojarrad, A.G. New Insights into the Influence of Weak and Strong Acids on the Oxidative Stability and Photocatalytic Activity of Porphyrins. *New J. Chem.* **2017**, *41*, 11053–11059. doi:10.1039/C7NJ02442H.

(24) Heydari-turkmani, A.; Zakavi, S.; Nikfarjam, N. Novel Metal Free Porphyrinic Photosensitizers Supported on Solvent-Induced Amberlyst-15 Nanoparticles with a Porous Structure. *New J. Chem.* **2017**, *41*, 5012–5020. doi:10.1039/C7NJ00791D.